HAL
open science

Co-grinding significance for calcium carbonate–calcium phosphate mixed cement. Part I: effect of particle size and mixing on solid phase reactivity

Solène Tadier, Nadine Le Bolay, Christian Rey, Christèle Combes

To cite this version:

Solène Tadier, Nadine Le Bolay, Christian Rey, Christèle Combes. Co-grinding significance for calcium carbonate–calcium phosphate mixed cement. Part I: effect of particle size and mixing on solid phase reactivity. Acta Biomaterialia, 2011, 7 (4), pp.1817-1826. 10.1016/j.actbio.2010.12.010 . hal-03544078

HAL Id: hal-03544078

https://hal.science/hal-03544078v1

Submitted on 26 Jan 2022

HAL is a multi-disciplinary open access archive for the deposit and dissemination of scientific research documents, whether they are published or not. The documents may come from teaching and research institutions in France or abroad, or from public or private research centers.

L'archive ouverte pluridisciplinaire **HAL**, est destinée au dépôt et à la diffusion de documents scientifiques de niveau recherche, publiés ou non, émanant des établissements d'enseignement et de recherche français ou étrangers, des laboratoires publics ou privés.

Open Archive TOULOUSE Archive Ouverte (OATAO)
OATAO is an open access repository that collects the work of Toulouse researchers and makes it freely available over the web where possible.

This is an author-deposited version published in : http://oatao.univ-toulouse.fr/
Eprints ID : 4644

To link to this article : DOI:10.1016/j.actbio.2010.12.010
URL : http://dx.doi.org/10.1016/j.actbio.2010.12.010

To cite this version : Tadier, Solène and Le Bolay, Nadine and Rey, Christian and Combes, Christèle (2011) *Co-grinding significance for calcium carbonate–calcium phosphate mixed cement. Part I: effect of particle size and mixing on solid phase reactivity.* Acta Biomaterialia, vol. 7 (n° 4). pp. 1817-1826. ISSN 1742-7061

Any correspondance concerning this service should be sent to the repository administrator: staff-oatao@inp-toulouse.fr.

Co-grinding significance for calcium carbonate–calcium phosphate mixed cement. Part I: Effect of particle size and mixing on solid phase reactivity

S. Tadier [a], N. Le Bolay [b], C. Rey [a], C. Combes [a,*]

[a] Université de Toulouse, CIRIMAT, UPS-INPT-CNRS, ENSIACET, 4 Allée Emile Monso, BP 44362, 31030 Toulouse Cedex 4, France
[b] Université de Toulouse, Laboratoire de Génie Chimique, UPS-INPT-CNRS, ENSIACET, 4 Allée Emile Monso, BP 44362, 31030 Toulouse Cedex 4, France

A B S T R A C T

In part I of this study we aim to evaluate and control the characteristics of the powders constituting the solid phase of a vaterite $CaCO_3$–dicalcium phosphate dihydrate cement using a co-grinding process and to determine their impact on cement setting ability. An original methodology involving complementary analytical techniques was implemented to thoroughly investigate the grinding mechanism of separated or mixed reactive powders and the effects on solid phase reactivity. We showed that the association of both reactive powders during co-grinding improves the efficiency of this process in terms of the particle size decrease, thus making co-grinding adaptable to industrial development of the cement. For the first time the usefulness of horizontal attenuated total reflection Fourier transform infrared spectroscopy to follow the chemical setting reaction at 37 °C in real time has been demonstrated. We point out the antagonist effects that co-grinding can have on cement setting: the setting time is halved; however, progress of the chemical reaction involving dissolution–reprecipitation is delayed by 30 min, probably due to the increased contact area between the reactive powders, limiting their hydration. More generally, we can take advantage of the co-grinding process to control powder mixing, size and reactivity and this original analytical methodology to better understand its effect on the phenomena involved during powder processing and cement setting, which is decisive for the development of multi-component cements.

Keywords:
Bone cement
Calcium carbonate
Calcium phosphate
Co-grinding
Particle size

1. Introduction

Calcium phosphate cements (CPC) for bone reconstruction have been the subject of intense research since they were proposed by Legeros et al. [1] and Brown and Chow [2] nearly 30 years ago. Their self-setting ability allows them to fulfil various requirements, including being placed in bony defects as a mouldable paste that sets and hardens in situ. This property has recently favoured the development of minimally invasive surgical techniques. Nevertheless, polymeric cements tend to be preferred to biodegradable and osteoconductive CPC for these applications, because of their ease of handling and injectability. It thus appears that there is a need to improve the formulations of mineral bone cements to meet surgeons' expectations, especially regarding higher cement resorbability, injectability, cohesion, radio-opacity and mechanical properties.

Many authors have in previous studies underlined the determinant effect of particle size and shape on the properties of CPC, such as viscosity of the paste [3–5], paste cohesion [5,6], injectability [3,7–9], setting time [3–7,10–12], cement porosity [3] and mechanical properties [3,5,6,8,13]. Moreover, studies have also proved the influence of other solid phase characteristics, such as interaction or/and agglomeration between particles [7,8]. Therefore, a possible way to improve the cement properties involves control of the solid phase physico-chemical characteristics, such as particle size distribution and morphology, powder mixing and interactions between reactants.

In this context, calcium carbonate–calcium phosphate mixed cements have recently been proposed and studied [14]. Compared with CPC, the high proportion of calcium carbonate that they contain should accelerate their resorption rate and favour bone ingrowth. The study presented herein deals with one of these cement formulations whose solid phase is composed of equal amounts of dicalcium phosphate dihydrate (DCPD) ($CaHPO_4{\cdot}2H_2O$) and $CaCO_3$ vaterite. These two powders differ not only in their chemical composition but also in the characteristics of the particles (morphology, size distribution, mean diameter and specific surface area).

In the field of biomedical hydraulic cements several studies have reported the use of dry grinding to prepare cement starting materials, and mechanochemical processes have been carried out to synthesise amorphous calcium phosphate or calcium-deficient hydroxyapatite (see, for example, [15]) to improve the reactivity of single or multi-component solid phase CPC and/or to mix it with organic additives [15–23]. In most of these studies the authors ground the reactive powders separately, often for a long period

* Corresponding author. Tel.: +33 5 34 32 3409; fax: +33 5 34 32 3499.
E-mail address: christele.combes@ensiacet.fr (C. Combes).

of time, mixed them, and then focused on the physical properties of the cement (mechanical resistance, injectability, rheological properties, etc.). However, the mixing process does not favour particle interactions, and good homogeneity is not necessarily obtained. While grinding has been used for a long time to reduce particle size, specific behaviors during co-grinding were only discovered in 1968 [24], since when this process has been used for the production of metallic alloys [25] and polymeric composites [26]. It has been shown that co-grinding not only reduces the filler size, but also increases the interactions between the particles [27]. Recently co-grinding has been used to produce porous biodegradable polymeric composite materials for bone tissue engineering [28], and it has been shown that this process enhances the mechanical resistance of the produced scaffolds.

As far as we know, a thorough examination of the mechanisms involved during cement solid phase grinding and the role of this process in activation of the separated or mixed reactive powders (grinding versus co-grinding) has not yet been carried out.

We aim to evaluate and control the characteristics of the particles constituting the solid phase (morphology, size distribution, median diameter, and specific surface area) using grinding and co-grinding processes and to determine their impact on the setting kinetics of vaterite $CaCO_3$–DCPD cement. The behavior of each powder component during grinding will first be investigated, followed by co-grinding of the solid phase (vaterite $CaCO_3$ and DCPD mixed together). Complementary characterisation techniques will be used to thoroughly analyse the various mechanisms involved during the vaterite $CaCO_3$ and DCPD grinding and co-grinding processes and to further understand their impact on the solid phase reactivity and setting ability of the vaterite $CaCO_3$–DCPD cement prepared with either unground, ground or co-ground powders.

2. Materials and methods

2.1. Reactive powder synthesis

The reactive powders constituting the solid phase of the cement (dicalcium phosphate dihydrate (DCPD) and vaterite ($CaCO_3$)) were synthesised by precipitation at ambient temperature. The protocols have been described in detail previously [14]. The precipitates were filtered (immediately for vaterite and after a maturation period of 5 h for DCPD), washed with deionised water, lyophilised, and stored in a freezer to prevent any evolution of these metastable powders before use.

2.2. Reactive powder grinding and co-grinding

Dry batch grinding and co-grinding experiments were performed using a laboratory tumbling ball mill in order to achieve the smallest particle size and a good powder mixture. It consisted of a 1 l alumina ceramic cylindrical chamber rotating around its horizontal axis and containing alumina ceramic balls of three different diameters: 19, 9.2, and 5.6 mm. There is an optimum ratio between the ball diameter and the particle size to obtain efficient grinding. Since the powder size decreases during grinding, the ball diameter must be adapted. Consequently, balls of different sizes are introduced into the chamber. The rotation speed of the chamber was fixed at 100 r.p.m., i.e. at 75% of the critical speed, while the ball loading volume represented 40% of the total volume of the chamber. These parameters were fixed at values commonly used in tumbling ball mills. The powder filling rate (10 g) represented 2% of the void space between the balls. This filling rate may be considered small compared with the usual rates used in industrial tumbling ball mills. In this study it was decided to minimise component consumption.

The powders were first ground separately. Then they were co-ground: a 1:1 weight ratio of brushite and vaterite powder mixture was co-ground to constitute the solid phase for $CaCO_3$–DCPD cement preparation. The 1:1 ratio of vaterite $CaCO_3$ to DCPD powder mixture is particularly interesting, as it has been shown to lead to a biphasic cement including biomimetic apatite and some remaining vaterite [14]. The latter is unstable under physiological conditions and thus its presence in the final cement composition can contribute to greater biodegradation and bioactivity of the cement.

Powder samples were taken from different regions of the mill chamber at various times for analysis. The sample mass removed at each time point was small enough (0.5 wt.%) not to significantly modify the proportion of powder in the mill. Immediately after removal the particle size distribution of the samples, expressed as the volume, was determined using a dry laser diffraction granulometer (Malvern Mastersizer 2000) and the median size $d_{0.5}$ corresponding to a cumulative percentage volume of 50% determined. The samples were stored in a freezer before being analysed by complementary techniques (scanning electron microscopy, Fourier transform infrared (FTIR) spectroscopy, X-ray diffraction, and specific surface area determination by the BET method).

The grinding and co-grinding study and measurements were performed in triplicate in order to check the reproducibility (on different batches) of these powder treatments.

Grinding and co-grinding processes were stopped just before the powders began to agglomerate, in order to achieve the smallest median size possible. The whole powder samples were then recovered, put in a hermetic flask and, as for the intermediate samples, stored in a freezer before physico-chemical analysis and their use for paste preparation, as presented below.

2.3. Paste preparation and setting kinetics

The cement paste was prepared by manually mixing either the unground, ground, or co-ground reactive powders (brushite and vaterite in equal amounts) with the liquid phase (deionised water) as previously published [14]. In every case the liquid to solid ratio (L/S) was equal to 0.5 (w/w). To let the cement set, the paste was then placed in a sealed container maintaining an atmosphere saturated with water and in an oven at 37 °C. The hardened and dried cements were analysed after maturation for 4 days at 37 °C.

Setting of the cement was followed as a function of time using a TAXT2 texture analyser (Stable Micro Systems) fitted with a cylindrical needle of 1 mm diameter (surface = 0.785 mm^2) that penetrates into the paste to a depth of 5 mm at a constant rate (2 mm s^{-1}). The setting time was considered to have been reached when the paste developed a maximum resistance to needle penetration of over 600 g mm^{-2} [29]. Each sample was analysed in triplicate.

The initial and final setting times were determined for the reference cement (prepared with the unground solid phase) according to a protocol adapted from the ASTM C266-03 and ISO 9917-1:2007 standards using a Gillmore needle apparatus HM-310 (Gilson Inc.). The characteristics of the Gillmore needle used to determine the final setting time corresponds to 514 g mm^{-2}, which is close to the value considered when using the method developed in our laboratory [32].

The chemical setting reaction of the cement was monitored using horizontal attenuated total reflection (H-ATR) FTIR spectroscopy (Nicolet 5700 spectrometer and Pike Technologies multi-reflections ZnSe crystal). Once prepared, the paste was placed on a ZnSe crystal, thermostated at 37 °C, and in contact with paper saturated with water to mimic the in use conditions. The FTIR spectrum was recorded every 5 min for 2 h.

The background spectrum was acquired using deionised water and subtracted for each sample spectrum.

2.4. Powder and cement characterisation

Unground, ground, and co-ground powders were characterised using FTIR spectroscopy (Nicolet 5700 spectrometer), X-ray diffraction (INEL CPS 120 diffractometer using a Co anticathode, $\lambda = 1.78897$ Å), specific surface area analysis by BET method (Monosorb MS-21, Quantachrom apparatus), and scanning electron microscopy (SEM) (Leo 435 VP microscope, sample silver plated before observation) techniques. The specific surface area of the powders was determined in triplicate.

3. Results

3.1. DCPD grinding

After synthesis DCPD crystals present a typical platelet morphology (see Fig. 1a). The median particle size determined by laser diffraction granulometry is 9.2 ± 0.3 μm.

Evolution of the size distribution and of the median size diameter of the particles of DCPD during grinding are shown in Fig. 2a and b, respectively. For better clarity we chose not to report all the size distributions in Fig. 2a.

With increasing grinding time the maximum of the particle size distribution curve is displaced towards smaller diameters due to particle abrasion and fragmentation. This result is confirmed by SEM observations of samples removed at different grinding times (Fig. 1b–d). These micrographs clearly show that abrasion of the particles (Fig. 1b–d) and formation of cracks (Fig. 1c) occurred. The latter phenomenon led to rapid fragmentation of the particles during the first 10 min of grinding (Fig. 1d).

These different phenomena are responsible for both the disappearance of larger particle populations and the formation of small fragments (Fig. 1d). As a result, the median particle size $d_{0.5}$ decreased rapidly during the first 10 min of grinding (see Fig. 2b). The DCPD initial median particle size was almost halved after 10 min grinding ($d_{0.5} = 5.1 \pm 1.0$ μm). Then this evolution slowed down, especially after 15 min grinding, and was quite stable after 25 min.

Fig. 1c and e shows that agglomeration phenomena involving interactions between smaller and bigger fragments begin to occur and thus compete with fragmentation, especially between 10 and 27 min grinding. During this period fragmentation and agglomeration phenomena lead to the formation of agglomerates of small fragments, as shown in Fig. 1c and e. Comparing the size distribution curves corresponding to 25 and 27 min grinding, we can see that at 27 min the curve tends more towards a small increase in larger particle proportions (as highlighted by the dotted circle in Fig. 2a). After 27 min grinding $d_{0.5}$ is 2.7 μm. Therefore, we chose to stop grinding DCPD at this time, as it corresponds to the optimal grinding time leading to the smallest DCPD median particle size while limiting the agglomeration phenomenon. Such DCPD powder treatment significantly increases the specific surface area (SSA): 3.04 ± 0.04 m^2 g^{-1} for DCPD ground for 27 min (see Table 1) compared with 1.30 ± 0.15 m^2 g^{-1} for the reference DCPD (unground DCPD).

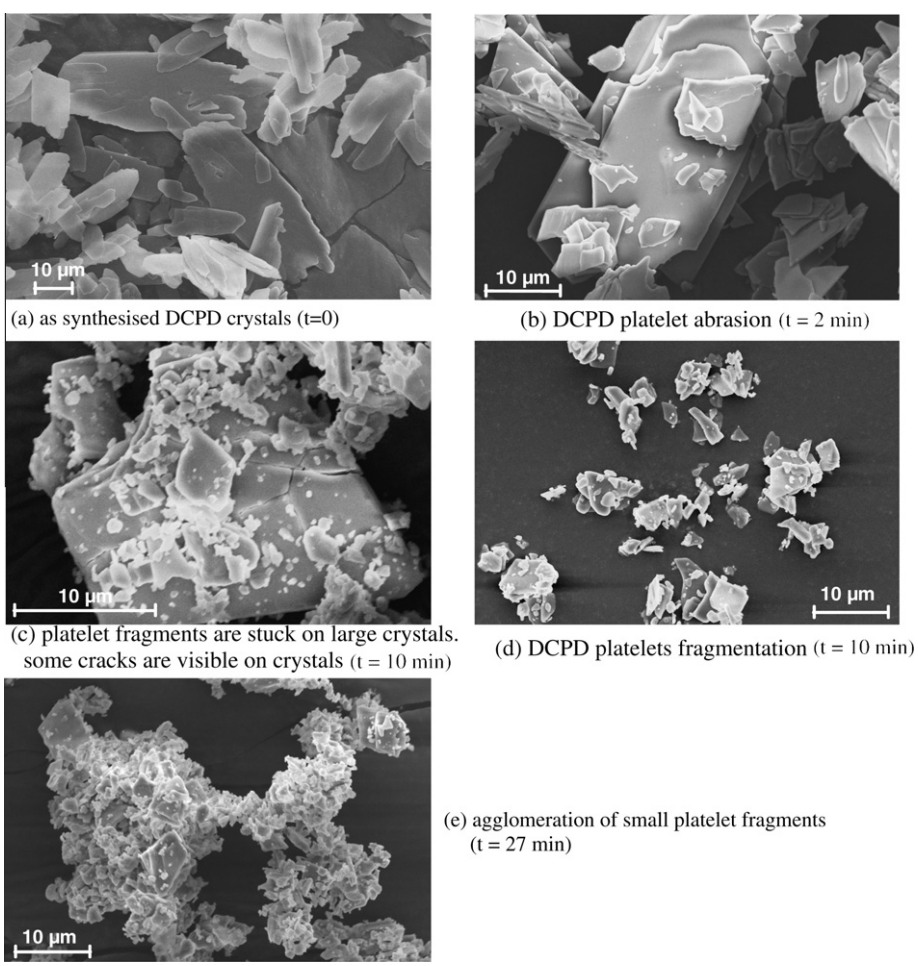

Fig. 1. SEM micrographs showing the morphological evolution of particles of DCPD during grinding.

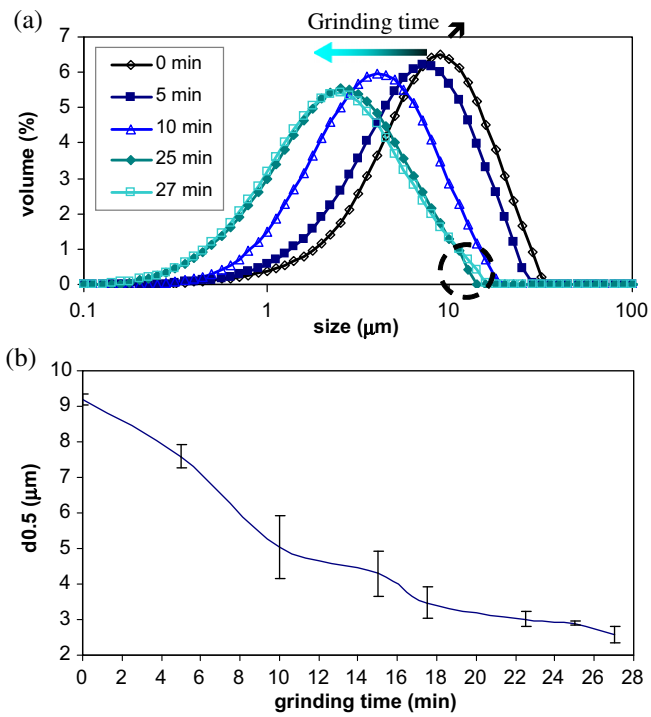

Fig. 2. Evolution of the DCPD particle size distribution (a) and median particle diameter (b) during grinding.

SEM observations indicated a significant decrease in DCPD particle size and an alteration in DCPD crystal morphology (a modification of the crystal aspect ratio) during the grinding process (Fig. 1a–e).

The FTIR spectra of unground DCPD and DCPD ground for 27 min presented in Fig. 3 show all the characteristic phosphate (524, 576, 789, 873, 985, 1058, 1132, and 1222 cm^{-1}) and water (661, 1650, 1724, 3166, 3277, 3491, and 3543 cm^{-1}) absorption bands of DCPD, indicating that DCPD was not transformed during grinding. In particular, we can note that during this high energy powder treatment no significant modification of the crystallisation and constitutive water content can be detected.

Complementarily, X-ray diffraction analyses of DCPD powders withdrawn after different grinding times show that the structure of the DCPD powder was unaltered by the grinding process (see Fig. 4), however, we note that the relative intensity of the (0 2 0) diffraction peak at $2\theta = 14°$ decreases dramatically as a function of grinding time. If we compare the intensity ratio of the (0 2 0) and (0 2 1) peaks as indicated on the X-ray diagram in Fig. 4 we can see that $I_{(020)}/I_{(021)}$ is seven times lower after 20 min grinding, indicating a significant change in DCPD crystal aspect ratio (length:width) and a decrease in preferential orientation, occurring especially when samples of thin elongated DCPD platelets (unground DCPD) (Fig. 1a) were prepared for XRD analysis. Thus, this phenomenon is less significant when using ground DCPD powder with more homogeneous particle dimensions (length and width) (Fig. 1d).

3.2. Vaterite grinding

Fig. 5 shows that the synthesised vaterite had crystallised as lentil-like particles. The median particle diameter determined by laser granulometry was $d_{0.5} = 1.7 \pm 0.1$ µm and the SSA was 36.8 ± 0.9 $m^2 g^{-1}$ (see Table 1). The particle size distribution presented as a function of grinding time in Fig. 6 shows no significant evolution after 4 min grinding. SEM observations confirm that vaterite particles were not fragmented during the grinding process and that their lentil-like morphology was retained (see Fig. 5b). In addition, the median particle diameter measured after 4 min grinding was equal to $d_{0.5} = 1.59 \pm 0.01$ µm, which is very close to the initial value. If we prolong the grinding treatment to 30 min, for example (see Fig. 6), a second mode appears in the size distribution at a larger particle size, and the first mode is broadened and slightly shifted towards a larger particle size due to agglomeration.

Vaterite grinding is inefficient and unuseful due to the low initial median particle size close to the size limit (around 2 µm), which has also been noted for other mineral compounds and cements [17,30,31].

Table 1
Specific surface area of the various powders and solid phases used to prepare the cement.

	DCPD	Ground DCPD (27 min)	Vaterite	Reference solid phase	Co-ground solid phase (13 min)
SSA_{BET} ($m^2 g^{-1}$)	1.30 ± 0.15	3.04 ± 0.04	36.8 ± 0.9	12.2 ± 0.7	8.1 ± 0.4

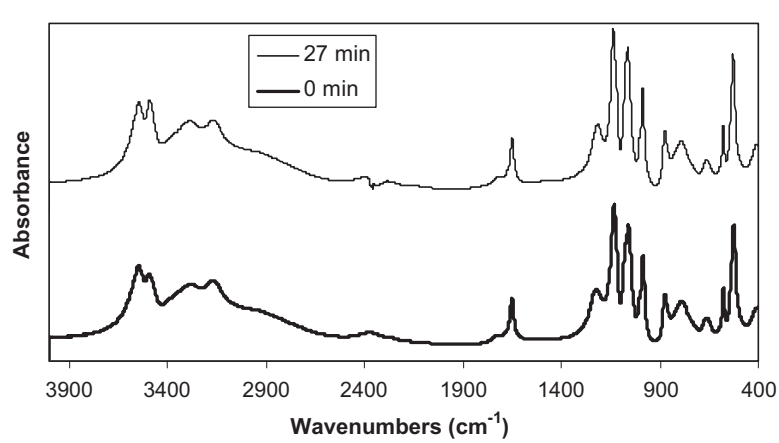

Fig. 3. FTIR spectra of DCPD before and after grinding for 27 min.

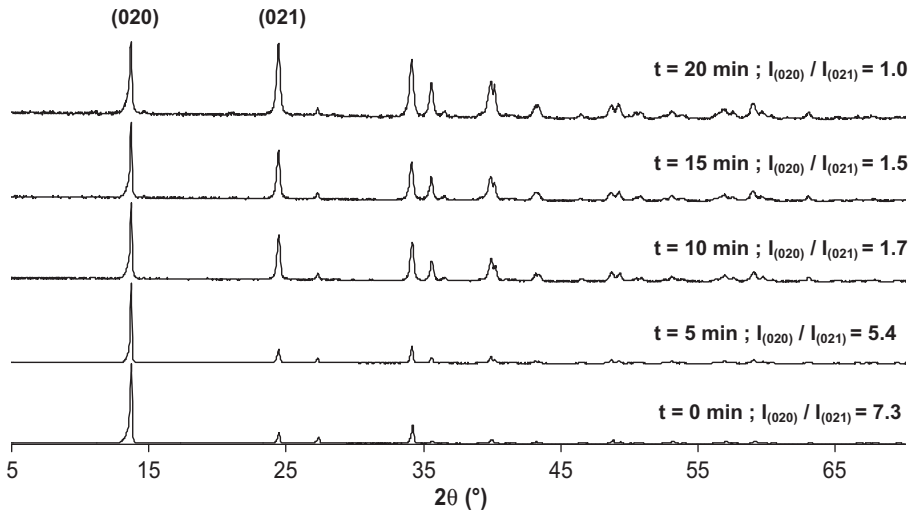

Fig. 4. X-ray diffraction diagram (Co anticathode, λ = 1.78897 Å) of DCPD after different periods of grinding: as-synthesised DCPD powder (t = 0 min) and after 5, 10, 15 and 20 min grinding.

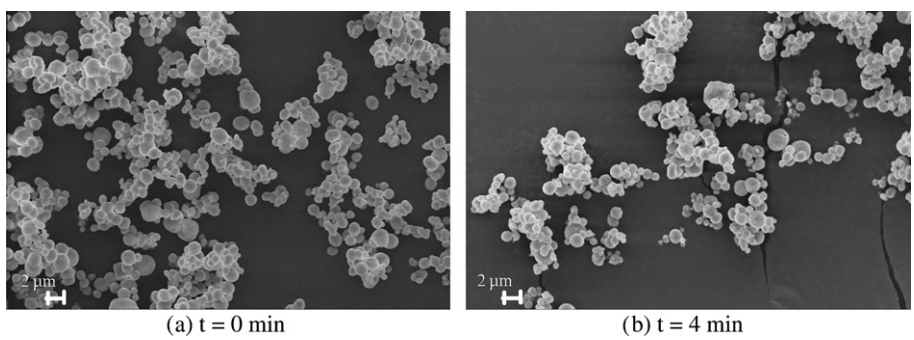

Fig. 5. SEM micrographs of vaterite particles before and after grinding (t = 4 min).

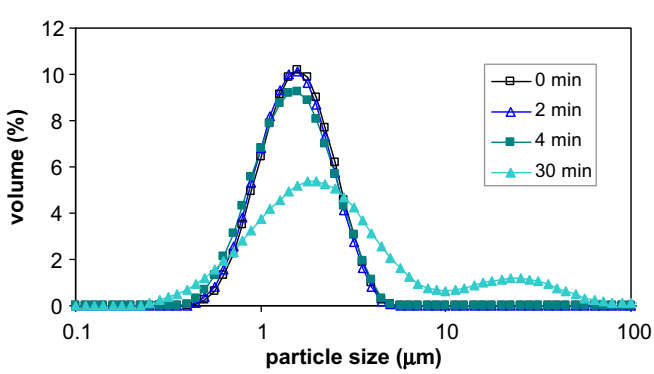

Fig. 6. Evolution of the vaterite particle size distribution during grinding.

X-ray diffraction and FTIR spectroscopy analyses allowed us to determine that there was no structural evolution of the vaterite when ground (data not presented).

The first part of this study has shown that vaterite and DCPD powders ground separately showed marked differences in behavior during the grinding process. In a second step we investigated the behavior of a vaterite $CaCO_3$–DCPD mixture during co-grinding.

3.3. Cement solid phase co-grinding

The evolution of the particle size distribution of the $CaCO_3$ vaterite–DCPD mixture (weight ratio 1:1) co-ground for different times is reported in Fig. 7a. The particle size distribution was initially bimodal, the two modes corresponding to DCPD (larger size) and vaterite (smaller size) particles. We note that during solid phase co-grinding the proportion of larger particles decreases, whereas the proportion of the smaller ones increases and the particle size distribution becomes broad and monomodal. Fig. 7b presents the evolution of the median particle size as a function of grinding time. We note that the decrease is fast, especially during the first 7 min of co-grinding, then slower until a size limit of 2.8 ± 0.1 µm is reached after 12 min co-grinding. The solid phase co-grinding time chosen for the rest of this study was 13 min, as it corresponds to the time to reach the smallest median particle size, before powders began to agglomerate. In addition, such short co-grinding times prevent partial transformation of vaterite into calcite, which could affect cement setting and properties (data not presented).

These results were confirmed by SEM observations (Fig. 8). Before co-grinding the vaterite $CaCO_3$ and DCPD powder mixtures show separate large DCPD platelets and small vaterite lentil-like particles (Fig. 8a). A thorough examination of the SEM micrographs of the vaterite–DCPD solid phase after different durations of co-grinding indicates that lentil-like vaterite particles tended to stick to larger DCPD particles (Fig. 8b–e). The latter were broken during grinding (Fig. 8d) and the small fragments resulting from this process showed more reduced particle sizes with increasing co-grinding time. Finally, alternation of fragmentation and agglomeration processes led to a mixture of both reactive powders (Fig. 8e and f). Thus the co-grinding process both reduces the particle size, especially of DCPD, and improves the homogeneity of the

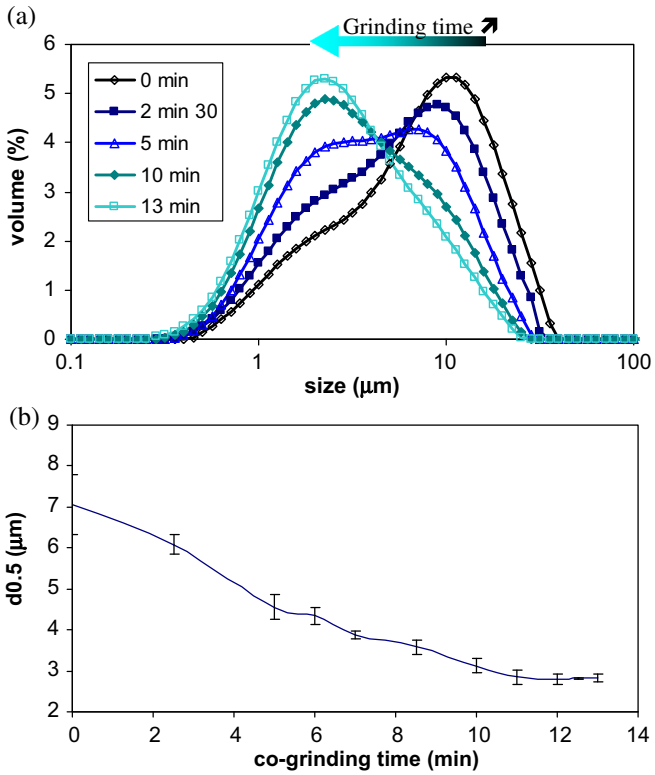

Fig. 7. Evolution of the size distribution and median size of the cement solid phase particles during co-grinding.

vaterite–DCPD mixture and interactions between both reactive powders: vaterite particles fully cover DCPD platelets crystals (Fig. 8e and f). After 13 min co-grinding the cement solid phase constituted a mixture of small reactive powder particles (Fig. 8e and f). SSA for the co-ground solid phase was $8.1 \pm 0.4\ m^2\ g^{-1}$ (see Table 1).

X-ray diffraction diagrams of the solid phase before and after 13 min co-grinding are presented in Fig. 9. No structural transformation of either reactive powder or additional phase can be detected. As already pointed out, on examining Fig. 4 for ground DCPD powders, the DCPD crystal aspect ratio and/or preferential orientation decreased ($I_{(020)}/I_{(021)}$ was lower after 13 min co-grinding), but did so less markedly for the co-ground solid phase (halved after co-grinding for 13 min; see Fig. 9) than for ground DCPD alone (one-fifth after 15 min grinding; see Fig. 4).

Regarding these results, we chose to co-grind the cement solid phase for 13 min to evaluate the benefit of this treatment for solid phase reactivity and, consequently, for some cement properties.

3.4. Setting reaction and time

X-ray diffraction diagrams of the hardened cement prepared either with the unground (reference) or co-ground solid phase are presented in Fig. 10, in comparison with rat bone. We note that solid phase pretreatment using co-grinding does not modify the composition and structure of the set cement, which in all cases was composed of an apatite analogous to bone mineral (broad diffraction lines characteristic of a nanocrystalline non-stoichiometric apatite) and some remaining vaterite [14,32]. The X-ray diffraction diagram obtained for the cement prepared with a solid phase containing ground DCPD was also analogous (data not presented).

The setting times determined for cement pastes prepared with either unground (reference) DCPD, ground DCPD, or co-ground solid phase are reported in Table 2. We note that co-grinding the reactive powders has a strong influence on the paste setting time, which is nearly halved when using the co-ground solid phase ($t_{setting} = 75 \pm 4$ min) compared with the reference cement ($t_{setting} = 140 \pm 2$ min). The use of ground DCPD in the cement solid phase also significantly reduced the setting time, but to a lesser extent ($t_{setting} = 90 \pm 5$ min).

We note that the final setting time of the reference cement determined according to the ASTM and ISO standards using a Gillmore needle apparatus (168 ± 7 min) confirmed good accordance with that determined according to a method using a texture analyser developed in our laboratory (Table 2). Indeed, it appears that we have underestimated the setting time by our method compared with the standard Gillmore needle method, due to the increase in needle penetration resistance as the needle penetrates the cement, whereas the needle remains on the cement surface when using the standard method.

FTIR spectroscopy in ATR mode allowed us to follow the cement setting reaction in real time, which could offer some additional data to explain the effects of solid phase co-grinding on cement setting.

The evolution of the FTIR spectrum (in the range 1270–820 cm^{-1}) of the reference cement paste (prepared with the unground reactive powders) as a function of time is reported in Fig. 11a. The characteristic vibration bands for hydrogenophosphate groups in DCPD (at 985, 1058, 1132, and 1222 cm^{-1}) and carbonate groups in vaterite (at 876 cm^{-1}), constituting the solid phase of the cement, are initially visible. The ν_3 PO_4 vibration band at 1020 cm^{-1} characteristic of apatite is visible as a marked shoulder after 30 min paste maturation; the relative intensity of this band increased strongly during the subsequent 2 h, confirming the formation of apatite as a product of the chemical setting reaction. We can see that the chemical setting reaction is incomplete after 2 h at 37 °C due to the presence of the characteristic vibration bands of hydrogenophosphate groups in DCPD, which are still visible, especially at 985 and 1132 cm^{-1} (Fig. 11a). Indeed, it lasts longer than 2 h, but these data are not presented because after 2 h the H-ATR FTIR signal is less intense due to the loss of close contact between the cement paste and the ZnSe crystal of the H-ATR FTIR system associated with paste shrinkage during setting.

If we compare Fig. 11a with b, which corresponds to the evolution of the FTIR spectrum (in the range 1270–820 cm^{-1}) of the cement paste prepared with the co-ground reactive powders, significant differences can be seen regarding progress of the setting reaction, especially during the first hour of paste evolution. Interestingly, 30 min after paste preparation the intensity of the band (shoulder) at 1020 cm^{-1} characteristic of apatite is lower than in the case of the reference cement. The marked difference in the 1020 cm^{-1} band intensity is also visible if we compare spectra obtained after 1 h (Fig. 11a and b), indicating a significant effect of co-grinding on the cement setting reaction kinetics. This effect is also marked when comparing the decrease in the intensity of the weak phosphate band of DCPD at 1222 cm^{-1} for both cements: a delay in the decrease in the intensity of this band is noted for cement pastes prepared with the co-ground solid phase, especially if we compare spectra corresponding to 1 h cement paste evolution (Fig. 11a and b).

4. Discussion

Several authors have studied in depth the dry mechanochemical synthesis of hydroxyapatite from DCPD and CaO reactive powders [15]. In particular, El Briak-BenAbdeslam et al. [15] reported a kinetic study showing that the amount of DCPD decreased exponentially with increasing grinding time, indicating that a

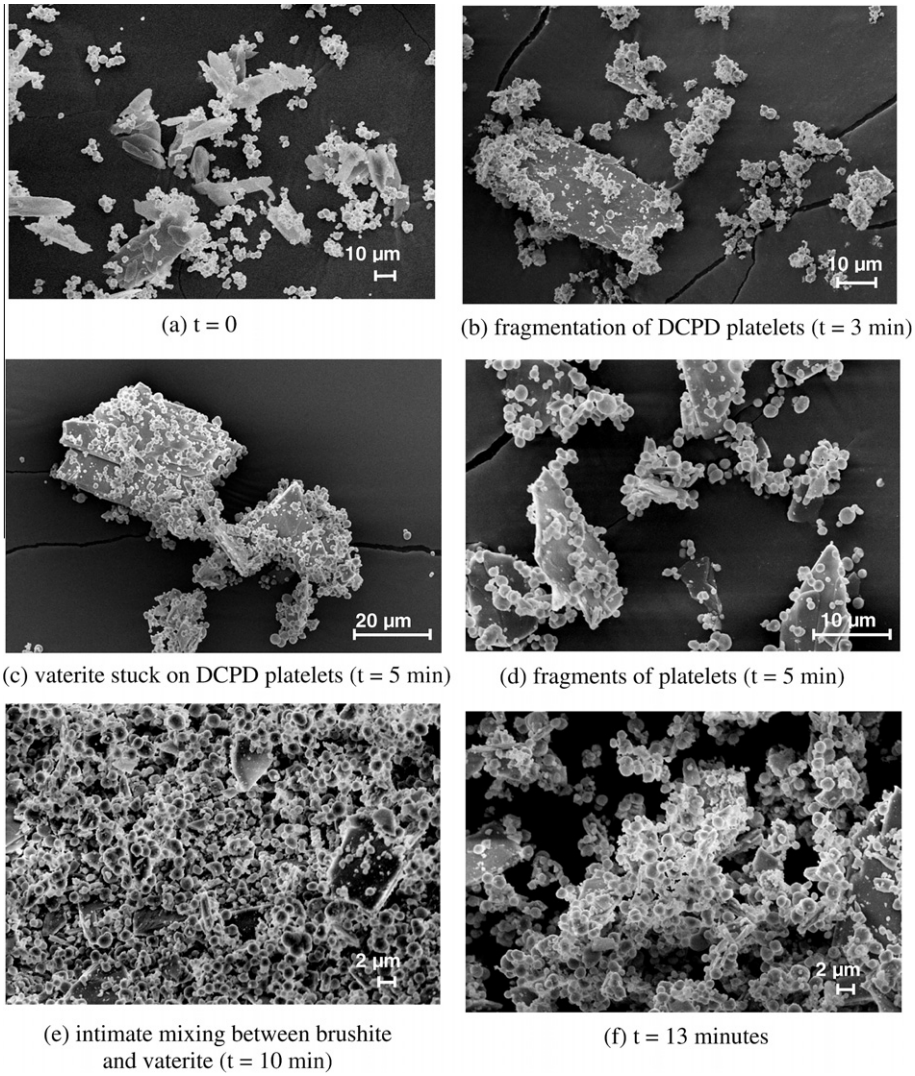

Fig. 8. SEM micrographs showing the evolution of the solid phase during co-grinding.

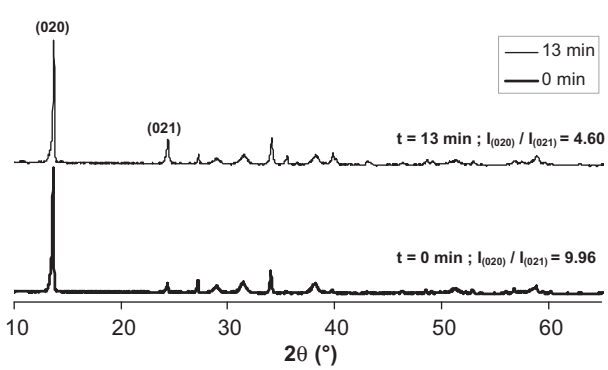

Fig. 9. X-ray diagram (Co anticathode, λ = 1.78897 Å) of the solid phase: unground (bold) and co-ground for 13 min.

DCPD–CaO reaction occurred, and they reported a decrease in the amount of DCPD of about 15% after 30 min grinding. The total disappearance of DCPD (completed reaction) occurred after 2 h grinding when 15 g of reactive powders were initially introduced [15]. The kinetics of the transformation of other calcium phosphate–CaO or calcium phosphate biphasic mixtures into hydroxyapatite using dry mechanical grinding was also investigated by Serraj et al. [16].

Gbureck et al. [17] showed that prolonged milling of β-tricalcium phosphate (TCP) (24 h) induced a phase transformation from the crystalline to the amorphous state, which in turn increased the solubility of TCP and accelerated the self-setting reaction leading to hydroxyapatite (accelerated setting time). In the case of high temperature bioceramics, Bignon et al. [33] indicated that prolonged milling of hydroxyapatite and TCP slurries led to re-precipitation of large particles of the most stable phase (hydroxyapatite), which in turn had an influence on the ceramic sintering, microstructure, and properties.

In our case, even if both reactive powders were metastable, no reaction between DCPD and vaterite was detected after 13 min co-grinding.

Most of the studies related to cement powder grinding have focused on particle size distribution analysis and determination of the specific surface area in discussing the effect of grinding on powder activation. This approach is sufficient to study single component cements [3,17,22]. In the case of multi-component cements, as in the present study, we consider other important analytical data, such as SEM observations, which, combined with granulometry analysis, allowed us to identify the various and

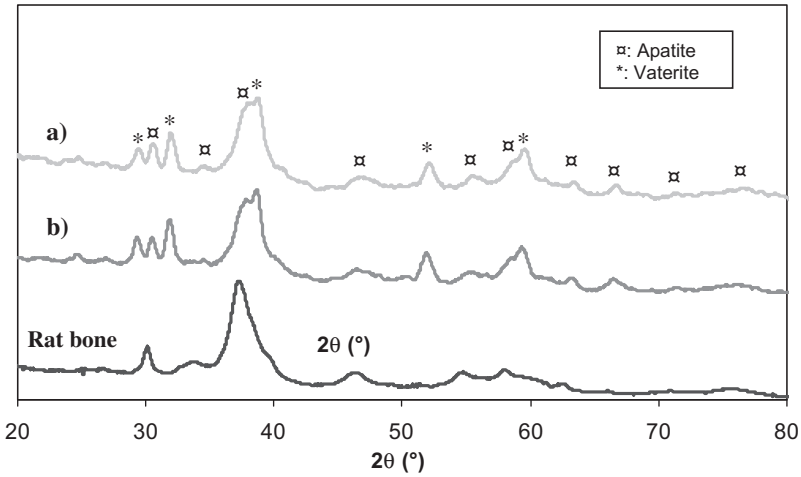

Fig. 10. X-ray diffraction diagram (Co anticathode, λ = 1.78897 Å) of the hardened and dried cement (after 4 days at 37 °C) prepared with (a) unground powders (reference cement) and (b) co-ground powders (vaterite and DCPD) compared with that of rat bone.

Table 2
Setting time of the cement prepared with unground (reference), ground DCPD or co-ground solid phase (determined using a texture analyser).

Cement solid phase	Setting time (min)
Reference	140 ± 2
Ground DCPD	90 ± 5
Co-ground solid phase	75 ± 4

successive mechanisms involved during vaterite $CaCO_3$–DCPD solid phase co-grinding. We have shown that co-grinding favours the fragmentation of large DCPD platelet crystals and close association of the two reactive powders (vaterite and DCPD) due to particle agglomeration.

A thorough study of the as-synthesised DCPD powder grinding behavior or of the vaterite $CaCO_3$–DCPD mixture co-grinding behavior showed that the minimum particle size was reached after a short period of powder treatment (<30 min). In all cases DCPD powder grinding or solid phase co-grinding involved a short period of pre-treatment: 27 or 13 min, respectively. These values were precisely determined by considering both the SEM and granulometry data to choose the duration of powder treatment, allowing a smaller particle size to be reached (even if the particles agglomerated) and the powder behavior during grinding or co-grinding to be understood. Interestingly, we note that the standard deviation for $d_{0.5}$ as a function of grinding time was significantly lower for solid phase co-grinding compared with DCPD grinding (comparison of the standard deviation reported in Figs. 2 and 7b) indicating a better control of particle size evolution by co-grinding (better repeatability and reproducibility) than grinding of DCPD.

Agglomeration always occurs during such high energy powder treatment and it appears more important to consider the individual particle size and avoid excessive agglomeration of particles to determine the optimum co-grinding time for the cement solid phase. Agglomeration has been reported by many authors based on an observed shift in particle size distribution toward larger particle sizes [4], but we have been unable to find studies in the literature on cement powders in which grinding time has been considered when investigating the mechanisms involved during this powder treatment.

As already reported in several papers, the present study has confirmed that the grinding process does not allow particle sizes under a few microns (typically 2 μm) to be achieved [17,31]. However, we have shown that this particle size limit is reached earlier when reactive powders are co-ground (after a shorter co-grinding time of t = 13 min, compared with 27 min grinding necessary for DCPD). The association of both reactive particles during co-grinding improved the efficiency of this process in terms of particle size decrease, thus making this process adaptable to industrial development of the cement.

Depending on the type of cement (single component, biphasic or multi-component), different effects/behaviors can be expected during and after grinding the reactive powders, which would control cement setting, chemical reactivity, and the mechanical properties. Several authors have proposed combining isothermal calorimetry data with particle size distribution analysis to better determine the reaction kinetics of tricalcium phosphate and brushite cements [22,34,35].

In the present study we have for the first time proposed a methodology by which to follow in real time the chemical cement setting reaction using H-ATR FTIR spectroscopy at 37 °C in an atmosphere saturated with water (Fig. 11). H-ATR mode FTIR spectroscopy offers additional advantages over the conventional transmission mode as analysis of the cement paste can be performed continuously in real time and in humid conditions, which also allows preservation of the hydrated layer on the surface of the nanocrystals of apatite. Rey et al. proposed that this hydrated layer is involved in biomimetic apatite cement setting, consolidation, and bioactivity [32].

The decrease in cement setting time combined with the delayed chemical reaction observed for cement prepared with a co-ground solid phase compared with a reference cement (see Table 2 and Fig. 11) is interesting. When using ground or co-ground powders an increase in the rate of the chemical setting reaction would have been expected, correlated with the decrease in setting time. Although it is difficult to distinguish the physical and chemical phenomena occurring during cement setting and hardening due to their superimposition, we hereafter propose considering them separately in order to discuss and try to explain the effect of co-grinding on the solid phase reactivity.

It has previously been shown that the setting reaction of this $CaCO_3$–DCPD cement composition is based on the chemical reaction of DCPD hydrogenophosphate ions with carbonate ions of vaterite according to the chemical reaction:

$$2HPO_4^{2-} + CO_3^{2-} \rightarrow 2PO_4^{3-} + CO_2 + H_2O$$

leading to a cement composed of a nanocrystalline carbonated apatite analogous to bone mineral (AB type carbonated apatite)

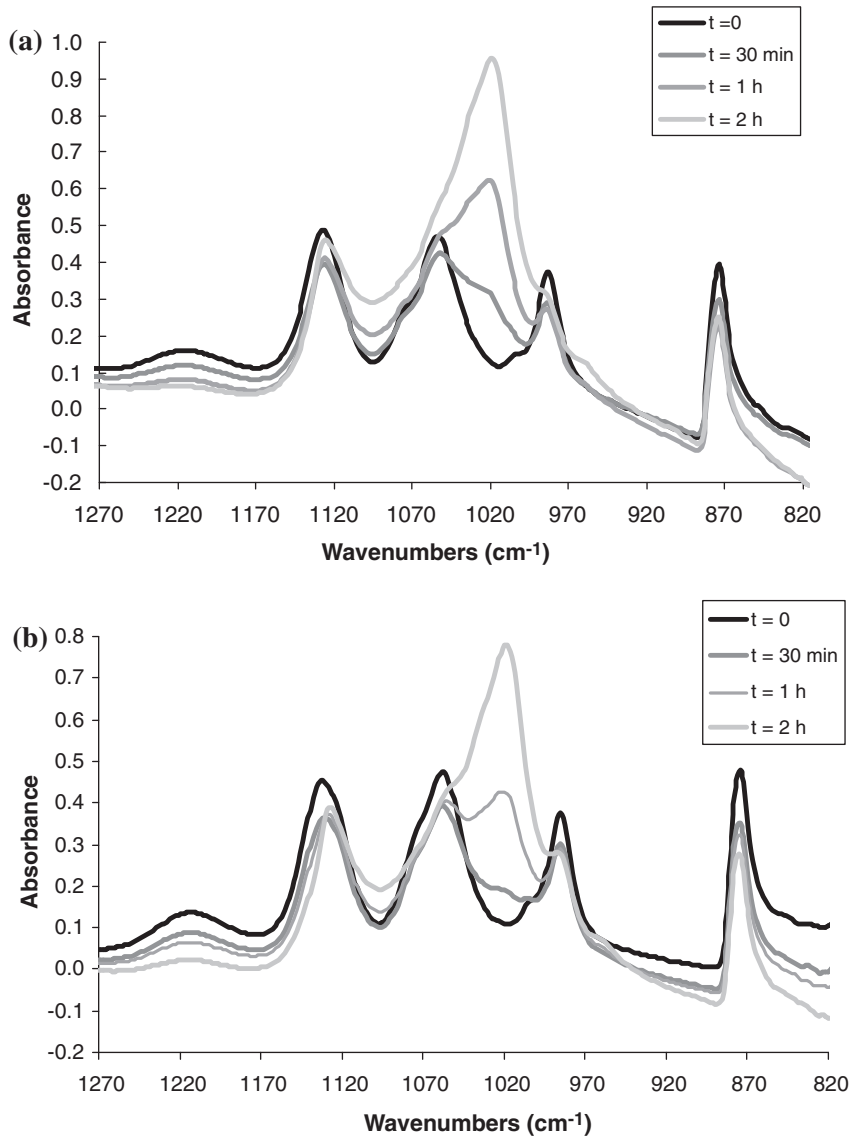

Fig. 11. Real time evolution of the FTIR spectrum of the cement paste at 37 °C for: (a) the cement paste prepared with unground solid phase; (b) the cement paste prepared with co-ground solid phase.

associated with untransformed vaterite $CaCO_3$ [14]. This reaction involves hydration of the reactive powders and a dissolution–reprecipitation process. As we have observed by SEM, when the reactive powders are co-ground the contact area between the DCPD and vaterite particles is increased, which in turn limits the surface area of both particles available to interact with water during the hydration process. In addition, it is well known that the latter controls the dissolution and, consequently, reprecipitation processes. Thus, the delay in co-ground powder hydration due to limited water accessibility could explain the delay of about 30 min in the dissolution of DCPD (in particular, a decrease in the 1222 cm^{-1} FTIR phosphate band characteristic of DCPD) and the formation of apatite (an increase in the 1020 cm^{-1} FTIR band characteristic of apatite) revealed on comparing Fig. 11a with b. The significantly higher specific surface area measured for the reference solid phase ($12.2 \pm 0.7\ m^2\ g^{-1}$) compared with that of the co-ground solid phase ($8.1 \pm 0.4\ m^2\ g^{-1}$) is consistent with this hypothesis (see Table 1).

In all cases the formation of apatite can be detected by ATR FTIR spectroscopy (phosphate band at 1020 cm^{-1}) from 30 min after paste preparation, which is well before the lowest setting time we measured (75 ± 4 min for the co-ground solid phase), indicating that the interaction of apatite nanocrystals, especially through the hydrated layer on their surface, is not the only phenomenon contributing to cement setting [32].

Some physical aspects also have to be considered. In particular, it is interesting to note that co-grinding of both reactive powders was more efficient in terms of setting rate than separate DCPD powder grinding. Several reasons can be put forward to explain these observations: (a) a decrease in the agglomeration of particles of the same nature; (b) homogeneity of the mixture compared with manual mixing; (c) an increase in contact area between the two reactive powders; (d) complexation between crystals/particles; (e) modification of the interactions between the two components, which has already been observed with other co-ground systems [19,27]. These phenomena should lead to an enhancement of the physical attractive forces between the reactive particles, which are also known to contribute to the initial cement strength and setting [5]. This study shows that the quality of powder mixing in terms of homogeneity and the interaction between reactive

particles is another important parameter which controls physical setting of the cement solid phase.

5. Conclusion

Grinding of the separate or mixed dry components of the biphasic cement solid phase vaterite $CaCO_3$–DCPD has been shown to be a means of controlling particle size and mixing, which in turn control physical (setting time) and chemical (reaction kinetics) setting.

We have shown that SEM observations combined with granulometry analysis allow the various and successive mechanisms involved during vaterite $CaCO_3$–DCPD solid phase co-grinding to be identified: co-grinding favours fragmentation of the large platelet-like crystals of DCPD and close association of the two reactive powders (vaterite and DCPD) due to particle agglomeration. The association of both reactive particles during co-grinding improves the efficiency of this process in terms of a decrease in particle size, thus making this process adaptable to industrial development of the cement. Furthermore, we have shown that co-grinding DCPD and vaterite powders can have antagonist effects on cement setting: the paste setting time is nearly halved compared with a reference (unground solid phase) cement, but the chemical setting reaction involving the dissolution of DCPD and formation of apatite is delayed by about 30 min, probably due to the increased contact area between the DCPD and vaterite particles, which in turn limits water accessibility and powder hydration.

This study has indicated the usefulness of co-grinding in controlling powder mixing, size and reactivity, which could have an effect on cement properties such as paste injectability and porosity and/or cement mechanical properties. A complementary study on the cement properties will be presented in another paper [36].

Finally, we can take advantage of the original analytical methodology presented in this study, especially, following the cement setting reaction in real time at 37 °C in an atmosphere saturated with water by H-ATR FTIR spectroscopy for the study of other mineral cements and/or self-setting systems.

Acknowledgement

The authors thank the Institut National Polytechnique de Toulouse for supporting this inter-laboratory research work (BQR INPT 2006).

Appendix A. Figures with essential colour discrimination

Certain figures in this article, particularly Figures 1, 2, 6 and 7, 8 are difficult to interpret in black and white. The full colour images can be found in the on-line version, at doi:10.1016/j.actbio.2010.12.010.

References

[1] Legeros RZ, Chohayeb A, Shulman A. Apatitic calcium phosphates: possible restorative materials. J Dent Res 1982;61S:343.
[2] Brown WE, Chow LC. Dental restorative cement pastes. US patent 4518430; 1985.
[3] Ginebra MP, Driessens FCM, Planell JA. Effect of the particle size on the micro and nanostructural features of a calcium phosphate cement: a kinetic analysis. Biomaterials 2004;25:3453–62.
[4] Baroud G, Cayer E, Bohner M. Rheological characterization of concentrated aqueous β-tricalcium phosphate suspensions: the effect of liquid-to-powder ratio, milling time, and additives. Acta Biomater 2005;1:357–63.
[5] Liu C, Shao H, Chen F, Zheng H. Rheological properties of concentrated aqueous injectable calcium phosphate cement slurry. Biomaterials 2006;27:5003–13.
[6] Bohner M, Gbureck U, Barralet JE. Technological issues for the development of more efficient calcium phosphate bone cements: a critical assessment. Biomaterials 2005;26:6423–9.
[7] Delgado JA, Harr I, Almirall A, del Valle S, Planell JA, Ginebra MP. Injectability of a macroporous calcium phosphate cement. Key Eng Mater 2005;284–286:157–60.
[8] Gbureck U, Spatz K, Thull R, Barralet JE. Rheological enhancement of mechanically activated α-tricalcium phosphate cements. J Biomed Mater Res B Appl Biomater 2005;73:1–6.
[9] Bohner M, Baroud G. Injectability of calcium phosphate pastes. Biomaterials 2005;26:1553–63.
[10] Brunner TJ, Grass RN, Bohner M, Stark WJ. Effect of particle size, crystal phase and crystallinity on the reactivity of tricalcium phosphate cements for bone reconstruction. J Mater Chem 2007;17:4072–8.
[11] Liu C, Shao H, Chen F, Zheng H. Effects of the granularity of raw materials on the hydration and hardening process of calcium phosphate cement. Biomaterials 2003;24:4103–13.
[12] Tofighi A, Palazzolo R. Calcium phosphate bone cement preparation using mechano-chemical process. Key Eng Mater 2006;284–286:101–4.
[13] Otsuka M, Matsuda Y, Suwa Y, Fox JL, Higuchi WI. Effect of particle size of metastable calcium phosphates on mechanical strength of a novel self-setting bioactive calcium phosphate cement. J Biomed Mater Res 1995;29:25–32.
[14] Combes C, Bareille R, Rey C. Calcium carbonate–calcium phosphate mixed cement compositions for bone reconstruction. J Biomed Mater Res 2006;79:318–28.
[15] El Briak-BenAbdeslam H, Mochales C, Ginebra MP, Nurit J, Planell JA, Boudeville P. Dry mechanochemical synthesis of hydroxyapatite from dicalcium phosphate dihydrate and calcium oxide: a kinetic study. J Biomed Mater Res A 2003;67:927–37.
[16] Serraj S, Boudeville P, Pauvert B, Terol A. Effect on composition of dry mechanical grinding of calcium phosphate mixtures. J Biomed Mater Res 2001;55:566–75.
[17] Gbureck U, Grolms O, Barralet JE, Grover LM, Thull R. Mechanical activation and cement formation of β-tricalcium. Biomaterials 2003;24:4123–31.
[18] Yu T, Ye J, Wang Y. Synthesis and property of a novel calcium phosphate cement. J Biomed Mater Res B Appl Biomater 2009;90:745–51.
[19] Yu T, Ye J, Gao C, Yu L, Wang Y. Effect of biomedical organic compounds on the setting reaction of calcium phosphates. Colloids Surf B Biointerfaces 2010;75:363–9.
[20] Wang X, Chen L, Xiang H, Ye J. Influence of anti-washout agents on the rheological properties and injectability of a calcium phosphate. J Biomed Mater Res B Appl Biomater 2007;81:410–8.
[21] Takagi S, Chow LC, Hirayama S, Sugawara A. Premixed calcium-phosphate cement pastes. J Biomed Mater Res B Appl Biomater 2003;67:689–96.
[22] Brunner TJ, Bohner M, Dora C, Gerber C, Stark WJ. Comparison of amorphous TCP nanoparticles to micron-sized α-TCP as starting materials for calcium phosphate cements. J Biomed Mater Res B Appl Biomater 2007;83:400–7.
[23] Romieu G, Garric X, Munier S, Vert M, Boudeville P. Calcium–strontium mixed phosphate as novel injectable and radio-opaque hydraulic cement. Acta Biomater 2010;6:3208–15.
[24] Benjamin JS. Dispersion strengthened superalloys by mechanical alloying. Metall Mater Trans B 1970;1:2394–951.
[25] Gilman PS, Benjamin UJS. Mechanical alloying. Ann Rev Mater Sci 1983;13:279–300.
[26] Pan J, Shaw WJD. Properties of a mechanically processed polymeric material. J Appl Polym Sci 1994;52:507–14.
[27] Zapata-Massot C, Le Bolay N. Effect of the mineral filler on the surface properties of co-ground polymeric composites. Part Syst Charact 2007;24:339–44.
[28] Le Bolay N, Santran V, Dechambre G, Combes C, Drouet C, Lamure A, et al. Production, by co-grinding in a media mill, of porous biodegradable polylactic acid–apatite composite materials for bone tissue engineering. Powder Technol 2009;190:89–94.
[29] Goncalves S. Élaboration d'un ciment phosphocalcique injectable: études physico-chimique, galénique et de biocompatibilité. PhD thesis. France: Institut National Polytechnique de Toulouse; 2001.
[30] Schönert K. Size reduction (fundamentals). Ullmann's encyclopedia of industrial chemistry, vol. B2, unit operations I. Weinheim: VCH Verlagsgesellschaft mBh; 1988. p. 5.1–5.14.
[31] Bohner M. Reactivity of calcium phosphate cements. J Mater Chem 2007;17:3980–6.
[32] Rey C, Combes C, Drouet C, Sfihi H, Barroug A. Physico-chemical properties of nanocrystalline apatites: implication for biominerals and biomaterials. Mater Sci Eng C 2007;27:198–205.
[33] Bignon A, Chevalier J, Fantozzi G. Effect of ball milling on the processing of bone substitutes with calcium phosphate powders. J Biomed Mater Res B Appl Biomater 2002;63:619–26.
[34] Bohner M, Malsy AK, Camiré CL, Gbureck U. Combining particle size distribution and isothermal calorimetry data to determine the reaction kinetics of alpha-tricalcium phosphate–water mixtures. Acta Biomater 2006;2:343–8.
[35] Hofmann MP, Nazhat SN, Gbureck U, Barralet JE. Real-time monitoring of the setting reaction of brushite-forming cement using isothermal differential scanning calorimetry. J Biomed Mater Res B Appl Biomater 2006;79:360–4.
[36] Tadier S, Le Bolay N, Girod Fullana S, Cazalbou S, Charvillat C, Labarrère M, et al. Co-grinding significance for calcium carbonate–calcium phosphate mixed cement. Part II. Effect on cement properties. J Biomed Mater Res Part B: Applied Biomater, submitted for publication.